

## OYSTER SHELL DISSOLUTION RATES IN ESTUARINE WATERS: EFFECTS OF pH AND SHELL LEGACY

GEORGE G. WALDBUSSER,<sup>1\*</sup> RYAN A. STEENSON<sup>2</sup> AND MARK A. GREEN<sup>3</sup>

<sup>1</sup>College of Oceanic and Atmospheric Sciences, Oregon State University, 104 COAS Administrative Building, Corvallis, OR 97331; <sup>2</sup>South Dakota State University, Brookings, SD 57006; <sup>3</sup>Division of Natural Sciences, St. Joseph's College of Maine, 278 Whites Bridge Road, Standish, ME 04084

**ABSTRACT** Oyster shell is a crucial component of healthy oyster reefs. Shell planting has been a main component of oyster restoration efforts in many habitats and has been carried out on scales from individual and grassroots efforts to multiagency efforts across entire estuaries. However, the cycling and lifetime of the shell that makes up the bulk of an oyster reef has only recently received attention, and most of the work to date has focused on the role of epi- and endobionts on shell degradation. Here we report findings from a laboratory study in which we manipulated pH in a flow-through control system using water from the mesohaline mouth of the Patuxent River to measure dissolution rates of intact oyster shell. Shells from the Eastern oyster (*Crassostrea virginica* Gmelin 1791) with three different legacies were exposed to 4 levels of pH that encompass a range typical of the mesohaline waters of the Chesapeake Bay (~7.2–7.9 on the NBS scale). Mass loss over a 2-wk period was used to measure dissolution rate on 3 shell legacies: fresh, weathered, and dredged. We found that pH and shell legacy had significant effects on shell dissolution rate, with lower pH increasing dissolution rate. Fresh shell had the highest dissolution rate, followed by weathered then dredged shell. Dissolution rates were significantly different among all 4 pH treatments, except between the lowest (~7.2) and the next lowest (~7.4); however, shells lost mass even under noncorrosive conditions (~7.9). We discuss the implications of our findings to ongoing efforts to understand shell budgets and cycling in oyster reef habitat, the interaction of biological and geochemical agents of shell degradation, and the complexity associated with shell carbonate cycling in the unique milieu of the oyster reef.

**KEY WORDS:** oyster shell, estuarine acidification, pH, oyster reef, biogeochemistry, calcium carbonate

### INTRODUCTION

The living oysters that make up the veneer of an intact oyster reef are supported by a framework of dead oyster shell (DeAlteris 1988, Hargis & Haven 1999), although the physical and chemical composition of interior oyster reefs have not been well quantified. Oyster restoration efforts have often focused on replanting dead oyster shell to help provide an initial framework on which oysters recruit. The role of this shell in supporting oyster growth has long been recognized as noted by the naturalist Pliny the Elder in his first-century work, *Natural History*. More recently, the importance of topographic relief in shell plantings has been shown, with taller shell plantings having greater success (Schulte et al. 2009). Although the importance of the shell habitat for recruitment of juveniles is well documented, the cycling of this shell material and lifetime on oyster reefs has only recently received treatment (Powell et al. 2006, Beck et al. 2009). Oyster shell is a dynamic resource on oyster reefs subject to a number of degradation processes that ultimately control the rate of loss from the reef. The integrated effect of physical, biological, and chemical processes degrading shell material over the time it spends in the outer reef layer determines how much of this material ultimately contributes to the reef framework versus being recycled to the water column.

A peculiar requirement of oyster reef health and growth is oyster mortality adding to the shell pool of the reef (Mann & Powell 2007, Southworth et al. 2010); in other words, for a reef to remain static with various degradation processes and effective sea level rise, it must have a healthy population of oysters with a mortality rate at least balancing the rate of shell loss

(Powell & Klinck 2007). Recent work in the Delaware River estuary has found that oyster shells on reefs have typical half-lives of years to a decade (Powell et al. 2006). Powell and Klinck (2007) argue that these loss rates should set the target population dynamics needed for self-sustaining populations. Although there are few estimates of shell lifetime from oyster reefs, the seemingly rapid rates from the Delaware suggest that oyster populations require a careful balance of recruitment, growth, and mortality to be self-sustaining (Mann & Powell 2007). Given the evidence that oyster recruitment is less consistent interannually and related to changes in environmental conditions such as salinity (Kimmel & Newell 2007), the processes affecting the lifetime of shells on oyster reefs have potentially important consequences for ongoing restoration efforts. In general, active breakdown of calcium carbonate hard parts is thought to occur in the taphonomically active zone (TAZ) (Davies et al. 1989), which occurs within the bioturbated and oxic zones of sediment seafloor. The important role of biont attack on shell persistence has been previously noted (Carver et al. (2010) and references therein), with shell-burrowing organisms such as polychaetes and sponges rapidly deteriorating oyster shell while it remains in the TAZ. Burial in anoxic conditions generally results in increased preservation (Hu et al. 2011) as a result of the exclusion of shell-boring organisms and ultimately more favorable geochemical conditions for calcium carbonate preservation (Morse 2005, Morse et al. 2007).

Although shell-boring organisms are often considered to be the primary agent of oyster shell degradation (Carver et al. 2010), the thermodynamics of surrounding estuarine waters sets the stage for stability of these biogenic minerals prior to burial. In addition, the pitting associated with fouling organisms changes the surface topography of shell material at small spatial scales (millimeters to centimeters), creating additional surface area

\*Corresponding author. E-mail: waldbuss@coas.oregonstate.edu.  
DOI: 10.2983/035.030.0308

where thermodynamic dissolution is thereby accelerated (Morse et al. 2007). The low salinity and high rates of production and respiration in many estuaries create conditions that may be transiently corrosive to the calcium carbonate of oyster shell. The calcium carbonate reef framework deposited by oysters in estuarine environments is therefore notable, given the less favorable thermodynamics compared with other reef-building organisms such as corals. Furthermore, oysters are prolific filter feeders, capturing organic matter from the water column and depositing it to the benthos, including their own reef framework. The deposited organic matter stimulates high rates of microbial metabolism contributing respired  $\text{CO}_2$ , increasing corrosiveness, and ultimately increasing dissolution of shell material until burial below the TAZ. Once buried below the oxic zone, however, this organic matter may, in fact, help preserve shell (Hu et al. 2011).

Adult and juvenile bivalves have been shown to deposit calcium carbonate under corrosive conditions, albeit at a reduced rate (Gazeau et al. 2007, Waldbusser et al. 2010, Waldbusser et al. 2011). After the organism dies, however, no new shell may be deposited, and the stability of the shell mineral is controlled by the corrosiveness of the surrounding conditions. Estuarine carbonate chemistry is variable with respect to many processes that alter the stability of calcium carbonate minerals, driven by production and respiration cycles (Abril et al. 2003, Borges & Gypens 2010, Feely et al. 2010, Waldbusser et al. 2011), freshwater input (Salisbury et al. 2008), and global changes in atmospheric  $\text{CO}_2$  (Miller et al. 2009). All have the potential to alter the lifetime of the calcium carbonate oyster reef building blocks in these thermodynamically unstable habitats, and all are susceptible to local and global human impacts.

The importance of calcium carbonate cycling to the global carbon cycle has precipitated significant research efforts on understanding the dissolution/preservation dynamics of the mineral phase (see reviews in Morse (2005) and Morse et al. (2007)) and the calcium carbonate counterpump in the world's oceans (Antia et al. 2001, Zondervan et al. 2001). However, within estuarine habitats, much less is known regarding the cycling of calcium carbonate and feedbacks with calcifiers. A recent analysis by Lebrato et al. (2010) found that echinoderm calcification on continental shelves is a small but significant component of the global carbon cycle. The short-term controls on and dissolution rates of these multicellular biogenic minerals have not been explored with much depth, particularly in relation to population dynamics and resource management timescales. However, taphonomic studies of longer term degradation rates (e.g., Kidwell 2005) and more recent experimental evidence from continental shelf environments provide some insight (Hu et al. 2011, Powell et al. 2011b).

One challenge to understanding these dynamics is that many estuarine calcifiers are multicell organisms producing shells that are heterogenous in nature with high preservation potential (of adult shells) even in relatively corrosive nearshore sediments. The calcium carbonate reaching the seafloor in the open ocean is often from single-cell organisms or small aggregates, whereas temperate estuarine calcifiers are frequently metazoans with large shells (and relatively small surface area (*sensu* Walter and Morse (1984)) already living on or within the sediment. Bivalve shells vary in mineral composition, proportion of organic matter, microstructure of mineral grains, and the outer organic sheath that protects the mineral component of the shell. These shell

characteristics all affect the rate at which shells dissolve resulting from thermodynamic conditions: corrosiveness of surrounding media. However, beyond a first-order thermodynamic argument, others have argued that factors such as biological interactions, bioenergetics of shell formation, and environmental variables ultimately determine the patterns and fate of shell material (Kidwell 2005, Hautmann 2006, Powell et al. 2011b). Shells undergo diagenetic transformation during burial, and that transformation alters surface chemistry and ultimately the dissolvability of the shell mineral. Formation of modified minerals called "micrite" resulting from dissolution and reprecipitation in marine sediments (Kobluk & Risk 1977, Longman 1980) results in elemental changes to the shell surface (Palma et al. 2008) as well as structural changes to the mineral crystallography. Ultimately, these early stages of transformation are the beginning of the fossilization of shell material. It is clear, therefore, that the legacy of the shell would likely impact the solubility under corrosive conditions, and these differences in legacy provide a snapshot into a time-variable component of shell dissolution on and within oyster reefs.

A combination of biological, geochemical, and sedimentary agents will ultimately affect the dissolution rates of intact shells in estuarine environments. To explore the role of estuarine geochemistry and shell characteristics on dissolution rates, we used a flow-through experimental  $\text{CO}_2$  system with feedback control to control pH and to measure dissolution rates of intact oyster shell over a 2-wk period. Specifically, our study addresses two primary questions: What is the response of the intact shell dissolution rate to a range of common estuarine pH values? What effect does shell legacy have on shell dissolution rates across these pH values? Furthermore, we explored the implications and mechanisms of dissolution rate response to these factors: pH and shell legacy.

## METHODS

### *Shell Collection*

Oyster shells of the species *Crassostrea virginica* were collected from three different sources resulting in three different shell legacies: fresh, dredged, and weathered. Fresh shells were obtained from a local oyster house in Solomons, MD, all meat was removed after shucking, and shells were placed into experimental conditions within 24 h of shucking. Dredged shells were collected from a marina in Stevensville, MD (Langenfelder Marine Inc.), which retained the shells from the State of Maryland dredged shell/oyster reef replenishment program. These dredged shells are sifted from dredge spoils around the Maryland portion of Chesapeake Bay and relocated to oyster restoration areas. Limited aging estimates of the dredged shell from the state of Maryland indicate the oldest shells are approximately 3,000 y BP, with many in the several-hundred-year range (C. Judy, MD-DNR, pers. comm. July, 25, 2011). Shells were collected haphazardly from a large shell pile at the marina, focusing on intact shells of a medium size relative to the rest of the shells in the pile. Weathered shells were originally collected from a local oyster house in Solomons, MD, shucked, and placed in a sandy, beachfront area for approximately 2 y. No differentiation was made between left and right valves of the shells for any of the legacies. The visual differences of the three shell types were obvious (Fig. 1). Fresh shells were generally smooth, and the

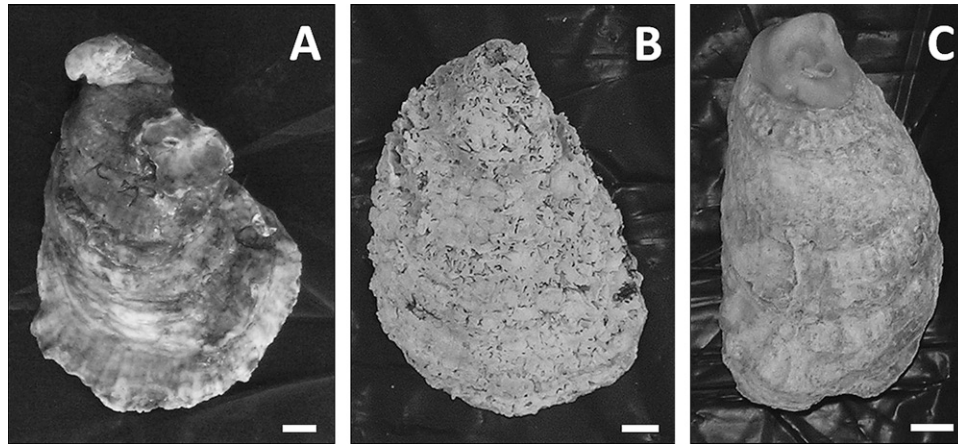


Figure 1. (A–C) Representative images of the 3 shell legacies used in the experiment: fresh (A), weathered (B), and dredged (C). White bars in each picture are 1 cm in length for scale.

outer shell appeared brown and generally had an intact periostracum. Dredged shells were whitish gray with some light secondary coloration of blue gray on a generally smooth surface. Weathered shells were white with extensive pitting on the order of a couple of millimeters in size on the shell exterior but not the interior. Some evidence of polychaete burrowing was found as black blisters on shell interiors of weathered and fresh shell.

#### pH Control System

A flow-through, feedback-control CO<sub>2</sub> manipulation system was used to control pH in the experimental system. The control system used was a Neptune Aquacontroller 3 (Neptune Systems, San Jose, CA) interfaced with a PC to record pH and temperature values every 2 min throughout the course of the experiment. Four epoxy filled, double-junction pH electrodes were used with an internal Ag/AgCl reference electrode, one within each treatment tank. Probes were calibrated with standard NBS buffers, rinsed and cleaned daily with deionized water, with the calibration checked daily against a standard 7.01 NBS buffer, and recalibrated at a minimum of once per week. During late July and early August 2009, incoming water from the seawater system of the Chesapeake Biological Laboratory was manipulated to obtain treatment levels (Table 1). The incoming water was drawn from the Patuxent River, a mesohaline tributary of the Chesapeake Bay. Throughout the course of the entire experiment salinity varied between 13–14 psu from daily measurements (with no measureable diurnal variability),

and temperature was recorded every 2 min with a mean and SD of  $27.28 \pm 0.48^\circ\text{C}$ , and a maximum and minimum of  $29.50^\circ\text{C}$  and  $23.80^\circ\text{C}$ , respectively. One hundred percent CO<sub>2</sub> was added in proportions to maintain an average pH (NBS scale) for 3 target treatments of 7.7 (high), 7.4 (mid), and 7.2 (low). Our actual values were 7.67, 7.38, and 7.17, each with an SD of 0.04 pH units throughout the entire course of the experiments, with values recorded every 2 min. These pH values were chosen to represent a range of conditions typical of the mesohaline region of the Chesapeake Bay. A control was also used in which incoming water was bubbled with ambient air to a pH set point of 7.90 with an SD of 0.04 during the experimental period. Bubbling was initiated when values dropped below the set point and was stopped when the set point was reached.

The experimental tank setup was designed to dampen diurnal variation in pH, allow for relatively constant carbonate chemistry, and provide constant flow rates to the experimental aquaria. Incoming water was plumbed to an open 20-L head tank in which river water entered the system, and flowed out from a standpipe to maintain a constant water level and thus head pressure of water fed to experimental aquaria. The water from the head tank was split to the 3 pH treatments and 1 control. Each treatment aquarium consisted of two connected 20-L containers, one for mixing and one for shells. A sheet of bubble wrap was placed on the surface water in both containers to minimize atmospheric exchange. Water and CO<sub>2</sub> were added to the mixing tank that was connected to the experimental tank by a short pipe. Water was cycled back to the mixing tank with a small submersible pump at a rate of roughly 54.4 L/h. The water in the experimental tank spilled over through an outlet, and the flow rate of water through each experimental aquarium (5.4 L/h) was controlled by a valve between the header tank and experimental tanks, and was checked daily and adjusted as necessary. At the volume of the experimental aquaria and target flow rates, the water had a residence time of roughly 8 h in experimental aquaria. We found the ratio of mixing flow to outlet flow (~10:1) resulted in the most stable controller response, and it limited cycling of pH in the experimental system. In addition, each experimental tank was situated on top of a small stir plate, and a magnetic stir bar was used to ensure complete mixing in the experimental tank where shells were suspended in a rack above the bottom of the tank

TABLE 1.

Average conditions ( $\pm 1$  SD) in experimental aquaria during the 2-wk measurement period.

	Temperature	Salinity	Alkalinity (mmol/L)	pH
Inlet	26.50 (0.62)	13.2 (0.4)	1.598 (0.014)	n/a
Control	27.28 (0.48)	13.2 (0.4)	1.604 (0.013)	7.90 (0.04)
High	27.28 (0.48)	13.2 (0.4)	1.613 (0.011)	7.67 (0.04)
Mid	27.28 (0.48)	13.2 (0.4)	1.686 (0.040)	7.38 (0.04)
Low	27.28 (0.48)	13.2 (0.4)	1.704 (0.053)	7.17 (0.04)

Values are pH units on the NBS scale.  
n/a, not applicable.

with several centimeters of space among the total of 15 shells per aquarium.

#### *Shell Weight and Surface Area*

The linear rate of decrease measured on individual shell mass was used to estimate dissolution rates for each shell. Five shells per shell legacy and pH treatment were placed in experimental conditions for 10 days prior to the experimental 2-wk mass loss period. Although we collected mass loss data during this initial 10-day period, we used this time to refine handling procedures of shells during weighing, and to allow shells to develop an initial biofilm. After the initial 10-day acclimation, mass loss estimates were based on a linear fit over a 2-wk period in which total mass of individual shells changed by as much as 2–3 g. The linear regression fit of mass loss over time for the experimental mass loss period was typically  $R^2 > 0.90$ ; thus, using the slopes of this relationship were valid for these short-term estimates of shell dissolution. Shells were weighed every 2–3 days by removing shells from treatment aquaria, blotting them dry, and allowing them to air dry for 15 min before measuring mass. This procedure was used because it was found to be reproducible and consistent in obtaining a wet weight of the shell mass without leading to complete drying of shells. Final dry weights of shells were obtained by drying for 24 h at 60°C, and were used to estimate the percent water content of shells.

The interior and exterior surfaces of all shells were photographed just prior to their placement into the experimental aquaria from a planar view on a black background to enhance contrast between shell and background. Shell interior and exterior surface areas were measured by using standard image analysis techniques (ImageJ 1.43u, National Institute of Health, Washington DC), and the measurement difference between interior and exterior surface area estimates was roughly 3%. Briefly, each image of 10 shells was imported into Image J, the color image was converted to a binary image, and the “analyze particles” command was used to compute the total surface area. Estimates of surface area were checked by examining the traces of shells relative to the original images. In some cases, because of the lack of contrast between shell edges and the background, shell edges had to be traced manually and the surface area estimates rerun on touched-up images.

#### *Alkalinity*

Alkalinity measurements of incoming and outflow waters for each pH treatment were measured at roughly 2 to 4-day intervals to ensure flow rates were sufficient to prevent alkalinity buildup resulting from shell dissolution. Alkalinity samples were taken from the water entering the experimental system and at the 4 drains from the experimental tanks. These measurements also permitted calculation of the saturation state of calcite at specific time points during the experimental period. Alkalinity was measured by a 2-point end point titration following Edmond (1970), and handled following best practices for open cell titration (Dickson et al. 2007). Samples were analyzed within 20 min of collection, and were kept in sealed syringes until the open cell titration was carried out. Alkalinity was used to calculate the calcite saturation state of the average conditions within the experiments using CO2SYS (van Heuven et al. 2011) with salinity-dependent dissociation constants from Millero et al. (2006).

#### *Electron Microprobe*

Elemental analysis of one representative shell from each legacy type in the control pH treatment was selected to determine whether shells from the different shell legacies had been significantly altered. Electron microprobe analysis of calcium, strontium, barium, manganese, iron, magnesium, aluminum, and silica on the interior and exterior shell surfaces, as well as a cross-section of the shell, was conducted. For each shell legacy, the left valve was used to eliminate differential effects between valves. Five replicate locations were analyzed on epoxy-embedded shell samples. Electron microprobe analyses of shells were performed at Oregon State University using a CAMECA SX-100 (CAMECA, Gennevilliers Cedex, France) instrument equipped with five wavelength dispersive spectrometers and high-intensity dispersive crystals for high-sensitivity trace element analysis. The shells were analyzed using a 15-keV accelerating voltage, a 50-nA sample current, and a 10- $\mu$ m beam diameter. Counting times ranged from 10 to 60 sec, depending on the element and desired detection limit. Data reduction was performed online using a stoichiometric PAP correction model (Pouchou & Pichoir 1984). Barium, manganese, and aluminum were below detection limits in all samples (FEI, Hillsboro, OR).

#### *Scanning Electron Microscopy*

Visual inspection of shell surfaces for diagenetic transformation was carried out by electron microscopy. Samples were taken from the same shells as the electron microprobe analyses by chipping a section of the outer shell surface. The shell samples were rinsed with deionized water and dried before sputtering with a Pb/Au layer. Samples were analyzed at the Oregon State University Electron Microscopy Laboratory under an FEI Quanta 600F scanning electron microscope.

#### *Experimental Design and Statistical Analyses*

A 2-way full factorial experimental design was used to examine the effects of shell legacy and pH (and their interaction) on dissolution rates of Eastern oyster shell. Five replicate shells of each shell legacy were randomly assigned to 1 of 3 pH treatments. Within each experimental aquarium, 15 shells total (5 of each legacy) were contained during the course of mass loss measurements. Percent mass loss per day was computed as the dependent variable by calculating the regression of mass over time for each shell (in grams per day), then dividing by the initial mass to determine a percent mass corrected dissolution rate for each shell in the experiment. The initial 2-way ANOVA found that the interaction effect of legacy and pH treatment was not significant, and it was therefore dropped from the analysis. Assumptions of ANOVA were checked by examining residuals visually against each independent variable, as well as by using Shapiro-Wilk's test of normality and Hartley's f-max test of heteroscedacity. Residuals were normally distributed for each treatment level within each factor (legacy and pH treatment). Assumption of homoscedascity was met for treatment levels within pH; however, variances were found to be significantly different among the three legacy treatments. To address this violation of assumptions, separate variance estimates were made for each shell legacy to be used in the treatment comparisons, and denominator degrees of freedom were computed using Satterthwaite's method for the subsequent ANOVA with variance groupings by shell legacy. All analyses were run in SAS v9.1.3 (SAS, Cary, NC).

## RESULTS

*Experimental System Performance*

The controller system maintained pH within experimental aquaria for the duration of the experiment, except for three failures that resulted in missing data (Fig. 2). Data were logged every 2 min from the 4 pH probes, and the SD of pH throughout the course of the experiment was roughly 0.04 pH units (Table 1). However, during three periods, the mid and low pH treatment controller circuit froze and no data were logged, as evident by the gaps in Figure 2. On examining the mass data for these periods of controller failure, there are no measurable deviations in the rate of mass loss relative to the overall trends. We recognize the potential pitfalls of the experimental system, but note that this appeared to have no significant consequence on the response variable during these controller blackouts.

*Shell Dissolution*

During the 2-wk period in which we measured mass loss of shells, we found significant overall effects of shell legacy ( $F_{2,35} = 42.94$ ,  $P < 0.0001$ ) and a positive effect of decreasing pH treatment ( $F_{3,28,6} = 50.90$ ,  $P < 0.0001$ ) on shell dissolution (Fig. 3). The pH values we used in these experiments are not atypical of conditions in this mesohaline section of the Chesapeake Bay, albeit only in a transient sense. All the pairwise comparisons were significantly different between shell legacies, and only the difference between the low and mid pH treatments was not significant (Table 2). Two of the five replicates in the fresh mid-pH group had dissolution rates higher than what would be predicted from the overall trends, thus driving the mean value up (Fig. 4). Closer examination of these shells (and several others) revealed visual evidence of polychaete burrows (black blisters on internal shell surfaces) and sponges (pitting on exterior shell surfaces) in the fresh shells, which corresponded to the higher dissolution rates. In general, linear model fits to the individual shell mass loss over time explained more than 90% of the variance in change in mass over time. The dredged/control-pH shells typically had the worst fits to a linear model because of the very small changes in mass during the experimental period. However, with decreasing pH and corresponding increases in dissolution rates, the linear fits increased, with the dredged low-pH shells all having an  $R^2$  value

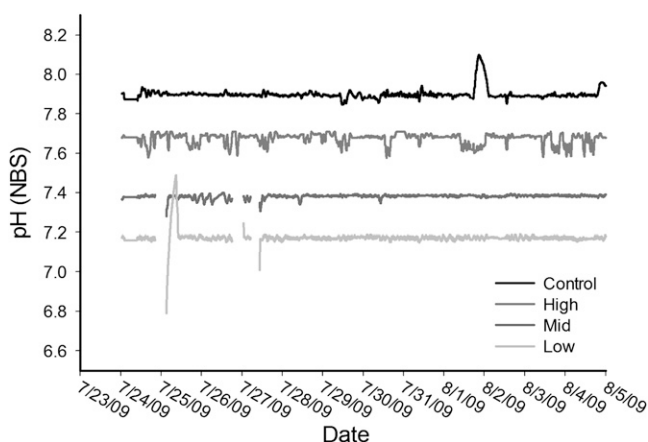


Figure 2. One hour centered mean pH values from each experimental tank.

of more than 0.95. We should also note that the patterns in shell dissolution rates are robust when standardized to planar surface area, rather than mass. Therefore, we will retain the units in per mass because they are in some ways easier to understand and to enable comparisons with estimates of shell half-lives.

The average percent water weights by shell legacy ( $\pm 1$  SD) at the end of the experiment were fresh,  $3.47 \pm 1.38$ ; dredged,  $1.90 \pm 1.71$ ; and weathered,  $5.06 \pm 3.63$ . A simple 1-way ANOVA found a significant effect of shell legacy on percent water weight ( $F_{2,32,1} = 11.60$ ,  $P = 0.0002$ ). Data were log transformed to meet assumption of normality, and variance was grouped by legacy because of unequal variance across the shell type. Significant differences, with Tukey-Kramer adjustment, were found between dredged and fresh shells ( $t_{33,6} = 3.76$ ,  $P = 0.0019$ ) and between dredged and weathered shells ( $t_{35,5} = 4.49$ ,  $P = 0.0002$ ), but not between fresh and weathered shells ( $t_{28,6} = 1.93$ ,  $P = 0.1457$ ). Note that the degrees of freedom vary among comparisons as a result of the Satterthwaite degrees of freedom estimation method used when grouping variance components.

*Alkalinity Measures*

Alkalinity values were used to determine saturation state for calcite (in conjunction with pH) and to ensure that flow rates were sufficient to prevent buildup of alkalinity in experimental aquaria. Water samples were taken from the inlet water supply and the outlet of the four experimental aquaria. The average inlet water alkalinity was  $1.60 \pm 0.01$  mmol/L. An increase in alkalinity over time was found in all treatments; however, our estimated error in the alkalinity measurements is roughly 0.015 mmol/L, and therefore is greater than the difference we found in the control, and equal to that in the high pH treatment. The differences between inlet and outlet waters for each pH treatment were control, below detection limit; high, 0.015 mmol/L; mid, 0.087 mmol/L; and low, 0.105 mmol/L. The increase of alkalinity in the low-pH treatment equates to a change in saturation state for calcite of 0.02, which highlights the minimal container effect of our system at the chosen flow rates. It should be noted here that remineralization of organic matter and release of nutrients generally decreases alkalinity, so these delta alkalinity values may be underestimating the true carbonate dissolution rate. Remineralization of organic components of the shell would contribute to the mass loss without an increase in alkalinity (and potentially a decrease depending on nutrient release rate). However, the organic components of oyster shell are generally less than 10% by weight. The different shell legacies were mixed in each pH treatment, thus the differences in alkalinity resulting from the dissolution of calcium carbonate are integrated across shell type. The average percentage (by weight) of shell material in each pH treatment was dredged, 25%; weathered, 33%; and fresh, 42%.

*Shell Elemental Analyses*

Shell elemental composition varied among the representative shell of each shell legacy (Fig. 5). Values presented in Figure 5 are from the inner shell surface of left (or bottom) valves only. Overall recoveries on analyses were generally near 100% on the weathered and fresh shells (indicating we captured nearly all the primary elements), but were as low as 80% on the dredged shell, implicating other possible elements for which we did not probe. The dredged shell had higher strontium concentrations on the inner shell surfaces and measurable concentrations of iron and

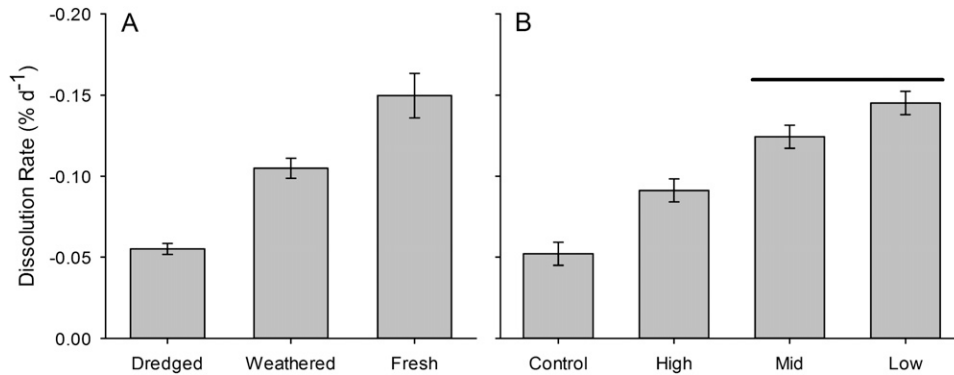


**Figure 3.** (A, B) Estimates of least square means for legacy (A) and pH treatment (B) effects. Error bars are SE estimates. Note that the different error estimates for the shell legacy means are the result of the individual variance estimates of these treatment effects.

silica, indicating early fossilization, whereas the fresh and weathered shell had lower strontium concentrations, and iron and silica concentrations below detection limits. A lower magnesium concentration was found on the weathered shell compared with other shell legacy types, indicating the preferential loss of the more soluble, higher magnesium calcite in the weathered shells (Morse et al. 2007, Burdige et al. 2010), subject to rainwater and terrestrial weathering processes. These limited data provide geochemical evidence of possible surface control on dissolution, and corroborate the electron microscopy observations below.

#### Visual Examination of Shell Surfaces

Examination of shell surfaces using electron microscopy highlights further differences in surface texture that likely have additional impacts on dissolution rates of different oyster shell. Figure 6 highlights three representative images of exterior shell surfaces of the same left valves used for electron microprobe analysis. The periostracum is visible on the fresh shell sample (Fig. 6A), with periostracal creases (white arrow) overlaid on the prismatic shell layer (black arrow). Breaks in shell growth are also visible, where edges of prisms are seen with growth occurring in the general lower left to upper right direction. The surface of the weathered shell (Fig. 6B) contains many small fragments and crystals occurring in various directions, indicating significant modification of the shell surface through the weathering process. The dredged shell surface (Fig. 6C) has

larger crystal formations, and some of the original prisms are also visible. These shells were buried in organic-rich sediments for significant periods of time; as a result, diagenetic cementing occurs (dissolution and reprecipitation) on the surfaces exposed to the corrosive sediments. It is again important to note that these images are from representative shells, and provide insight (not conclusive evidence) into the possible role of microstructure and surface processes in controlling dissolution rates of intact shells of differing legacies.

#### DISCUSSION

Our laboratory-based measurements of intact oyster shell dissolution highlight the potential role of environmental changes in carbonate chemistry on this important and limiting estuarine resource. Across a typical range of pH values for this mesohaline region of the Chesapeake Bay, the rate of shell dissolution changed significantly (Figs. 3 and 4). In addition, the legacy of the shell had equally important consequences on the dissolution rate, altering the dissolution rate by about a factor of 10 from the slowest dissolving dredged shells to the more rapidly dissolving fresh shells (Figs. 3 and 4). The short timescale (weeks) of this

**TABLE 2.**

**Results from pairwise comparisons among treatments within each factor of the 2-way ANOVA.**

Pairwise Comparisons	df	t Value	Adjusted P value
<b>Shell legacy</b>			
Dredged vs. fresh	21.1	6.69	<0.0001
Dredged vs. weathered	28.1	7.11	<0.0001
Fresh vs. weathered	26.2	2.97	0.0144
<b>pH treatment</b>			
Control vs. high	28.6	4.86	0.0002
Control vs. mid	28.6	8.96	<0.0001
Control vs. low	28.6	11.55	<0.0001
High vs. mid	28.6	4.10	0.0017
High vs. low	28.6	6.69	<0.0001
Mid vs. low	28.6	2.59	0.0677

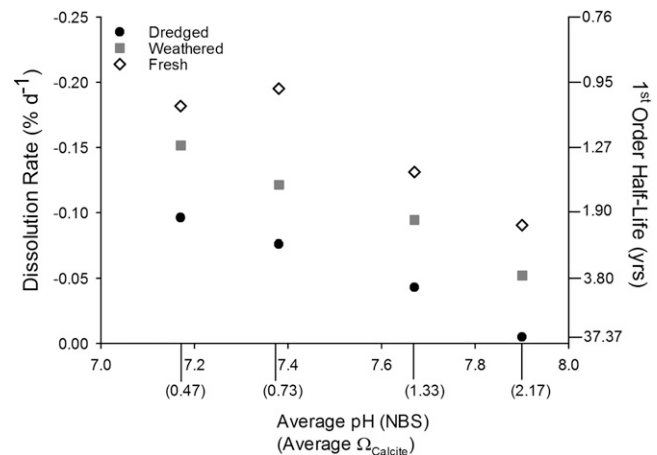


**Figure 4.** Average dissolution rates of individual treatments related to pH. The saturation state for calcite is presented below the pH values for reference. On the right y-axis are the first-order half-life values computed from the rate constants measured during the experiments. It is important to note the measurements are instantaneous rate constants for a short window of time, roughly 2 wk (see text).

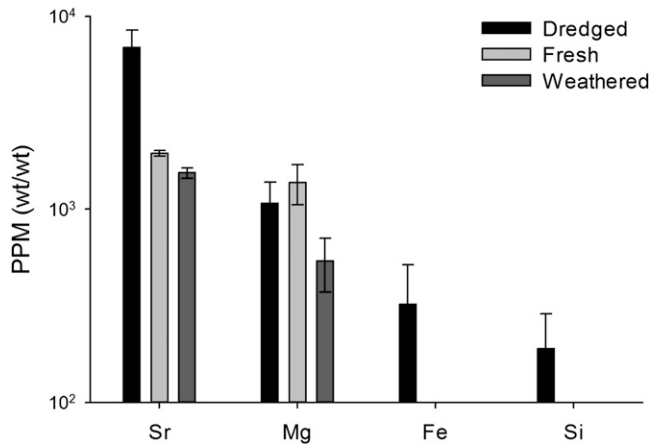


**Figure 5.** Trace element composition of interior shell surfaces in parts per million (PPM). Iron and silica were less than detection limits on the dredged shell cross-section analysis of the interior shell, and strontium in this region was also similar to that of the fresh and weathered shells.

experiment provides a snapshot of dissolution rates in response to changes in estuarine carbonate chemistry, but excludes other factors that are also responsible for shell degradation, such as shell-boring organisms. Although we noted evidence of shell-boring organisms, none were present on or in the shells during the experiment. Our measured rates in these short-term experiments are, however, within the range of other previous measurements of shell degradation. In an early study of shell dissolution Hecht (1933) showed that, immediately after death, mollusc shells may lose 25% of their mass in a matter of weeks. Driscoll (1970) found mass loss rates of up to 16% per year of shells in Buzzard's Bay, MA, attributed largely to boring organisms. Our measurements of dissolution (excluding bionts) range from roughly 2 to 70% per year, depending on shell type and pH (Fig. 4). This extrapolation to per year for any of our pH values has obvious limitations given the multiple scales of variability in estuarine carbonate dynamics. The most appropriate application of these rate loss values would be to apply to variable pH records of sufficient temporal resolution, such as hours, and integrate rate loss over longer periods of time, thus providing an estimate of geochemical shell loss to estuarine pH. However, if pH values for a given timeframe are normally distributed, using the average pH would provide an adequate estimation. Our experiments were conducted at a narrow range of temperature and salinity—factors important to carbonate thermodynamics. Our experiments do indicate that oyster shell lifetime, within the more surficial and open parts of a reef,

may be susceptible to changing estuarine carbonate chemistry, and is supported by recent work in shelf environments on shell breakdown (Hu et al. 2011, Powell et al. 2011a).

#### *Shell Half-Life and Agents of Destruction*

Shell dissolution rates may be used to compute shell half-lives to evaluate the role of pH and carbonate chemistry in maintaining/degrading oyster reefs. Recent estimates of Eastern oyster shell half-lives on reefs by Powell et al. (2006) indicate that in the Delaware Bay estuary shell half-lives range from just older than 1 to ~20 y, with the shortest half-lives found in mesohaline waters. Fitting our loss rates to an exponential decay model (as in Powell et al. (2006)), the shortest half-lives we compute are roughly 1 y for fresh shell under mid and low pH, and increase to nearly 40 y in the dredged control pH treatment (Fig. 4). It is important to note half-life increases exponentially with decreasing rate loss, and applied to our experimental data, shell lifetime is therefore most sensitive to changes in the upper pH range. After rate losses drop roughly  $0.05 \text{ d}^{-1}$  (or roughly  $20 \text{ y}^{-1}$ ), half-lives increase very rapidly, identifying a possible threshold type response of shell to degradation/dissolution rates. The rates of fresh shell decay in our experimental range are well above this threshold, and extrapolating linearly to higher pH values finds that this  $0.05 \text{ d}^{-1}$  rate would be obtained at a pH of 8.25 for the fresh shells in our experiment. The estimates and extrapolations from our experiments only account for geochemical degradation and exclude effects from shell-boring organisms (e.g., Zuschin et al. 2003, Carver et al. 2010).

In Chesapeake Bay, Pomponi and Meritt (1990) found that 90% of oyster shells were infested with a boring sponge, and these values were not unusual compared with other estuarine habitats (Rosell et al. 1999). Several of the fresh shells in our experiments had visual indicators of biont attack prior to the experiment, with visible black blisters on interior shell surfaces from polychaetes and bore holes from sponges (although no organisms were found in or on shells). Some of the highest dissolution rates we measured on individual shells were in the mid-pH treatment, with evidence of endobiont attack, and evidence of biont attack generally resulted in higher dissolution rates within pH treatment groups of fresh shells.

In the Delaware estuary, however, Powell et al. (2006) noted that the shortest half-lives were found in mesohaline waters, where boring sponges generally decrease in abundance with decreasing salinity (Hopkins 1962). Mesohaline estuarine environments are, however, often the region of chlorophyll maxima (such as in the Delaware River (Mannino & Harvey 1999)), and thus higher

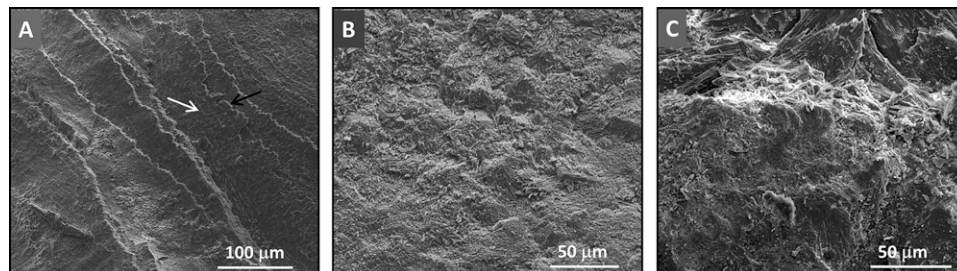


**Figure 6.** Representative scanning electron micrographs of the 3 shell legacies, outer shell surfaces of the left valves. (A) Fresh shell legacies. The white arrow notes the prisms in the prismatic layer, whereas the black arrow highlights a periostracal crease. (B) Weathered shell legacies. (C) Dredged shell legacies.

rates of production and respiration should result in a greater diurnal range in pH. Coupled with the lower alkalinity buffering in these environments, the overnight respiration signal is likely to create corrosive conditions for calcium carbonate minerals. We are not arguing that biont attack on shell is trivial, rather that biological and geochemical agents likely work in tandem, by creating microzones of respired CO<sub>2</sub> and additional surface area for dissolution. Should continued anthropogenic impacts on estuarine ecosystems result in less thermodynamically favorable estuarine conditions for calcium carbonate (Abril & Frankignoulle 2001, Borges & Gypens 2010, Feely et al. 2010, Waldbusser et al. 2011), shell budgets may be increasingly controlled by geochemical processes.

#### *Time Dependency of Shell Degradation and Shell–Reef Dynamics*

The comparison of the fresh shell with the other two shell types provides possible insights into the time dependency of shell degradation rates (noted by Powell et al. (2011a)) and highlights shell cycling dynamics on oyster reefs. Few studies of the physical and geochemical structure of an oyster reef exist, from the outer layer to the interior core (Davies et al. 1989, Hargis & Haven 1999). An important, and peculiar, requirement for an oyster reef to grow is the mortality of oysters and contribution of their shell to the reef framework (Powell et al. 2006, Mann & Powell 2007)—a framework composed of shell, organic deposits, and pore space in poorly constrained proportions. The rates of fresh shell dissolution we measured may be representative of shells during the early postmortality stage. However, as shells age (on a growing reef), they are eventually buried, presumably in an anoxic environment closer to the reef interior, thus excluding biont attack, and in a generally more favorable geochemical environment for preservation of calcium carbonate (Hu et al. 2011). Also during this transition from the near reef surface to reef interior, the exterior of the shell undergoes early diagenetic alteration, altering the surface chemistry of the calcium carbonate mineral and ultimately solubility (Morse & Arvidson 2002).

If the reef interior is in fact a diffusion-limited environment, the shell surface will dissolve and reprecipitate, leading to a less soluble surface for dissolution. Our dredged shell measurements, therefore, may represent a shell after having undergone this early diagenesis and then subsequently having been reexposed to oxic conditions. Thus, the differences in dissolution rate from the fresh to dredged shell may be, to some degree, an estimate of end members in a time-dependent dissolution rate. Furthermore, it is important to note that should the shell be buried within the reef framework, it would be exposed to a very different geochemical milieu. Decreases in reef accretion rates resulting from decreased oyster population growth, or increases in erosion resulting from changed hydrographic conditions could result in exposure of older/deeper more modified shells, perhaps providing a feedback in shell budget as a result of the lower dissolution rates of previously buried shell.

#### *Importance of the Shell Dissolution Surface*

Evidence from elemental analyses and electron microscopy of representative shells highlights the importance of surface control on dissolution rates under these moderately corrosive conditions (Morse & Arvidson 2002). Elevated concentrations of silica and iron on the dredged shell surface (Fig. 5) suggest the initial stages of diagenetic transformation (Longman 1980, Palma

et al. 2008) and micrite formation (recrystallized calcium carbonate) have altered surface characteristics. Elevated silica and iron values have been measured previously in outer prismatic layers (Carriker et al. 1991) and are similar to our measurements of foliated interior shell surfaces (Fig. 5), but aluminum was below detection limits, providing us with confidence that we captured foliated microstructure. Our electron microscopic images further support that the dredged shells were in an early stage of diagenetic transformation rather than sampling different microstructures, based on the larger crystal shapes seen in Figure 6C. Larger crystal sizes (and thus less surface area for dissolution) can be generated by dissolution and reprecipitation without altering chemical composition of the mineralogy (Morse & Casey 1988), and/or result in new mineral formation (Rude & Aller 1991). The geochemical and visual evidence of shell surface alteration are suggestive of both processes and, coupled with our dissolution rate measures, highlight the disconnect between bulk mineral properties and dynamics of mineral dissolution (Morse & Arvidson 2002), particularly of intact shells in estuarine environments.

Our study shows that even in supersaturated conditions, with respect to calcite, shells decreased in mass. The remineralization of organic shell components is one likely explanation for this response (Glover & Kidwell 1993), especially given the fact that the fresh shells had the highest dissolution rates (and the most organic material). However, organic components of oyster shell are typically a small percentage. The presence of a surface for microbes to colonize, and the secondary effects of metabolic CO<sub>2</sub> production (Emerson & Bender 1981) and microzone dissolution (Berner 1969) on shell surfaces are likely also at play.

The rates of shell dissolution we measured here are more than an order of magnitude lower than modeled calcite dissolution estimates in the open ocean seafloor (Hales & Emerson 1997). Much of the intact shell mass is not available to dissolve because of the low surface area-to-volume ratio of an oyster shell relative to a calcite grain (Walter & Morse 1984). Although others have examined the differences in calcium carbonate dissolution among biogenic and authigenic minerals, and the differences in available surface area (Cubillas et al. 2005), this work has been done on crushed shell. For example, assuming a perfect spherical calcite grain of 0.2 mm in diameter, one can calculate the mass per surface area as roughly  $1.4 \times 10^{-3}$  g/cm<sup>2</sup>, whereas the mass per surface area we measured for shells was 0.854 g/cm<sup>2</sup>. Our planar surface area measurements do not account for curvature of shells and microtexture, but do highlight the importance of this basic geometric comparison in regulating shell dissolution. Clearly, there are many dynamics modulating the dissolution of intact oyster shell. Our measurements simply set the stage for determining the magnitude of response to changes in estuarine pH.

#### *Oyster Reefs and Estuarine Calcium Carbonate Dynamics*

Oyster reefs are significant biogenic carbonate masses in thermodynamically variable and often unstable estuarine environments. To date, most interest in carbonate dissolution has focused on the seafloor of continental shelves and the open ocean (Honjo & Erez 1978, Cai et al. 2006, Hu et al. 2011) because of the important role of these habitats in global carbon cycling. Significant carbonate dissolution has been found in nearshore marine sediments (Green & Aller 1998, Green & Aller 2001) and estuarine turbidity maximum zones (Abril et al. 2003). The role of keystone species such as seagrass, algae, or corals on carbonate cycling in



coastal environments has also been highlighted (Gattuso et al. 1996, Bensoussan & Gattuso 2007, Burdige et al. 2008), but these studies have generally focused on carbonate-rich tropical environments. Postlarval juvenile and adult oysters can precipitate calcium carbonate in thermodynamically unfavorable conditions (Gazeau et al. 2007, Waldbusser et al. 2011) and, coupled with a high rate of organic matter deposition, this shell material may be readily preserved if buried quickly enough. In an insightful treatment, Kidwell and Jablonski (1983) noted the significant of sediment “shelliness” and positive ecological feedbacks of shell to changing benthic community composition (termed “taphonomic feedback”). If the responses of oyster shell dissolution to changing pH we measured (Figs. 3 and 4) were reasonable estimates of *in situ* conditions, then changes to estuarine geochemistry may be an important factor for oyster restoration.

Estuarine carbonate chemistry is dynamic, however, with many processes occurring across multiple temporal and spatial scales, including production/respiration cycles (Abril et al. 2003, Borges & Gypens 2010), hydrologic and watershed changes (Salisbury et al. 2008, Najjar et al. 2010, Aufdenkampe et al. 2011), and eutrophication (Gypens et al. 2009, Feely et al. 2010, Waldbusser et al. 2011). The importance of shell to the estuarine ecosystem (Gutierrez et al. 2003, Powell et al. 2006, Kelly et al. 2011, Green et al. accepted), the dynamic biogeochemistry in these environments, and feedbacks of shell budgets with population dynamics suggest (Powell et al. 2006, Mann & Powell 2007) this is an important and challenging area of future research.

#### *Managing Shell Resources*

One interesting note with regard to the dredged shell is that it had been used extensively by the state of Maryland to restore previously harvested oyster reefs from 1960 until 2006. Approximately 196 million bushels of dredged oyster shell were replaced in Chesapeake Bay during this 46-y period from the program's inception to termination (MD DNR). This is likely the largest coordinated shell planting/reef restoration effort to date, and also perhaps the largest alkalinity buffering experiment conducted. From a kinetic perspective, the use of dredged shell may have helped provide additional benefits from its lower rate of dissolution under all pH conditions (Figs. 3 and 4). The slower dissolution rate may have been especially beneficial during the early time frame of shell planting when carbonate conditions may have been less favorable for calcium carbonate preservation (Aufdenkampe et al. 2011). This potentially lower loss rate resulting from dredged shell meant that the population size needed to provide shell through mortality could have been smaller, helping to balance the shell budget (Powell et al. 2006). However, it is unknown whether these potential benefits also translate into a lesser degree of biont attack, and how the overall shell budgets were altered by the planting of dredged shell. At the control pH value, the dredged shell had a half-life 10 times higher than the fresh shell or, a loss rate equivalent to fresh shell at a pH of roughly 0.2 pH units lower. Although the shell planting

program has been discontinued, in part because of the lack of accessible shell, and it may be difficult to reconstruct previous shell budgets, the likely significant positive effect this effort should not be overlooked (Southworth et al. 2010).

A recent analysis has suggested that oysters are “functionally” extinct because of their precipitous decline in numbers relative to former populations (Beck et al. 2009). Thus the ecosystem functions (e.g., filtering, habitat) that oysters provided in the past have been lost. With ongoing restoration efforts aimed at restoring shells to former oyster grounds in many regions, understanding the controls on the lifetime of shells and how they relate to anticipated changes to estuaries from local and global anthropogenic impacts seems crucial. Conversely, changing the balance of shell material in estuaries may also have significant geochemical implications (Waldbusser et al. in prep). Shell planting may be a worthwhile mitigation strategy for some bivalves (Green et al. 2009); however, without the characterization of oyster population dynamics (Harding et al. 2010, Southworth et al. 2010) needed to provide renewed shell, these activities may be less effective than anticipated. The susceptibility of oyster shell and other bivalve shells in shell beds to dissolution extends beyond simple first-order thermodynamics arguments (Kidwell 2005); however, these first-order processes are important to constrain rate losses and to provide a starting point for understanding how shell resources in estuaries will respond to future anthropogenic impacts, including harvest and changing biogeochemistry. Our study provides limited, but important, insight into the possible future of oyster shell cycling. Relatively small increases in acidity may require shell replacement rates higher than can be achieved by natural populations and, vice versa, relatively small decreases in acidity could help provide natural oyster populations with an advantage. The geochemical control on dissolution of oyster shell needs to be evaluated in the context of other biological and sedimentary processes that ultimately control the lifetime of oyster shell on the reef.

#### ACKNOWLEDGMENTS

We acknowledge the Research Experience for Undergraduates (REU) program supported by Maryland Sea Grant and the National Science Foundation for supporting R. A. S. to carry out this research. This work was also supported by NSF-OCE#0622999 to M. A. G. and G. G. W. We thank Langenfelder Marine Inc. for allowing us to pick shells from their dredged shell pile, Frank J. Tepley at Oregon State University for carrying out the electron microprobe analyses, Liu Yi at Oregon State University for assistance with electron microscopy, and Bud Millsaps at the Chesapeake Biological Laboratory for his assistance with the seawater system. G. G. W. thanks Chris Judy and Eric Weissberger at the Maryland Department of Natural Resources for information on the Maryland shell planting program, Janet Nye for data on biological oxygen demand of Patuxent River waters, and Sarah E. Kolesar and Eric Powell for comments on a previous version of this manuscript.

#### LITERATURE CITED

- Abril, G. & M. Frankignoulle. 2001. Nitrogen-alkalinity interactions in the highly polluted Scheldt basin (Belgium). *Water Res.* 35:844–850.
- Abril, G., H. Etcheber, B. Delille, M. Frankignoulle & A. V. Borges. 2003. Carbonate dissolution in the turbid and eutrophic Loire estuary. *Mar. Ecol. Prog. Ser.* 259:129–138.

- Antia, A. N., W. Koeve, G. Fischer, T. Blanz, D. Schulz-Bull, J. Scholten, S. Neuer, K. Kremling, J. Kuss, R. Peinert, D. Hebbeln, U. Bathmann, M. Conte, U. Fehner & B. Zeitzschel. 2001. Basin-wide particulate carbon flux in the Atlantic Ocean: regional export patterns and potential for atmospheric CO<sub>2</sub> sequestration. *Global Biogeochem. Cycles* 15:845–862.
- Aufdenkampe, A. K., E. Mayorga, P. A. Raymond, J. M. Melack, S. C. Doney, S. R. Alin, R. E. Aalto & K. Yoo. 2011. Riverine coupling of biogeochemical cycles between land, oceans, and atmosphere. *Front. Ecol. Environ.* 9:53–60.
- Beck, M. W., R. D. Brumbaugh, L. Airoidi, A. Carranza, L. D. Coen, C. Crawford, O. Defeo, G. J. Edgar, B. Hancock, M. Kay, H. Lenihan, M. W. Luckenbach, C. L. Toropova & G. Zhang. 2009. Shellfish reefs at risk: a global analysis of problems and solutions. Arlington, VA: The Nature Conservancy. 52 pp.
- Bensoussan, N. & J.-P. Gattuso. 2007. Community primary production and calcification in a NW Mediterranean ecosystem dominated by calcareous macroalgae. *Mar. Ecol. Prog. Ser.* 334:37–45.
- Berner, R. A. 1969. Chemical changes affecting dissolved calcium during bacterial decomposition of fish and clams in sea water. *Mar. Geol.* 7:253.
- Borges, A. V. & N. Gypens. 2010. Carbonate chemistry in the coastal zone responds more strongly to eutrophication than to ocean acidification. *Limnol. Oceanogr.* 55:346–353.
- Burdige, D. J., X. Hu & R. C. Zimmerman. 2010. The widespread occurrence of coupled carbonate dissolution/reprecipitation in surface sediments on the Bahamas Bank. *Am. J. Sci.* 310: 492–521.
- Burdige, D. J., R. C. Zimmerman & X. Hu. 2008. Rates of carbonate dissolution in permeable sediments estimated from pore-water profiles: the role of sea grasses. *Limnol. Oceanogr.* 53:549–565.
- Cai, W. J., M. H. Dai & Y. C. Wang. 2006. Air–sea exchange of carbon dioxide in ocean margins: a province-based synthesis. *Geophys. Res. Lett.* 33. DOI: 10.1029/2006GL026219.
- Carriker, M. R., C. P. Swann, R. S. Prezant & C. L. Counts. 1991. Chemical elements in the aragonitic and calcitic microstructural groups of shell of the oyster *Crassostrea virginica*: a proton probe study. *Mar. Biol.* 109:287–297.
- Carver, C. E., I. Theriault & A. L. Mallet. 2010. Infection of cultured Eastern oysters *Crassostrea virginica* by the boring sponge *Cliona celata*, with emphasis on sponge life history and mitigation strategies. *J. Shellfish Res.* 29:905–915.
- Cubillas, P., S. Kohler, M. Prieto, C. Chairat & E. H. Oelkers. 2005. Experimental determination of the dissolution rates of calcite, aragonite, and bivalves. *Chem. Geol.* 216:59–77.
- Davies, D. J., E. N. Powell & R. J. Stanton. 1989. Relative rates of shell dissolution and net sediment accumulation: a commentary: can shell beds form by the gradual accumulation of biogenic debris on the seafloor. *Lethaia* 22:207–212.
- DeAlteris, J. T. 1988. The geomorphic development of wreck shoal, a subtidal oyster reef of the James River, Virginia. *Estuaries* 11:240–249.
- Dickson, A. G., C. L. Sabine & J. R. Christian, editors. 2007. Guide to best practices for ocean CO<sub>2</sub> measurements. *PICES Spec. Publ.* 3: 191 pp.
- Driscoll, E. G. 1970. Selective bivalve shell destruction in marine environments: a field study. *J. Sediment. Petrol.* 40:898.
- Edmond, J. M. 1970. High precision determination of titration alkalinity and total carbon dioxide content of sea water by potentiometric titration. *Deep-Sea Res.* 17:737.
- Emerson, S. & M. Bender. 1981. Carbon fluxes at the sediment–water interface of the deep sea: calcium carbonate preservation. *J. Mar. Res.* 39:139–162.
- Feely, R. A., S. R. Alin, J. Newton, C. L. Sabine, M. Warner, A. Devol, C. Krembs & C. Maloy. 2010. The combined effects of ocean acidification, mixing, and respiration on pH and carbonate saturation in an urbanized estuary. *Estuar. Coast. Shelf Sci.* 88:442–449.
- Gattuso, J. P., M. Pichon, B. Delesalle, C. Canon & M. Frankignoulle. 1996. Carbon fluxes in coral reefs. 1. Lagrangian measurement of community metabolism and resulting air–sea CO<sub>2</sub> disequilibrium. *Mar. Ecol. Prog. Ser.* 145:109–121.
- Gazeau, F., C. Quidlier, J. M. Jansen, J. P. Gattuso, J. J. Middelburg & C. H. R. Heip. 2007. Impact of elevated CO<sub>2</sub> on shellfish calcification. *Geophys. Res. Lett.* 34. DOI: 10.1029/2006GL028554.
- Glover, C. P. & S. M. Kidwell. 1993. Influence of organic matrix on the postmortem destruction of molluscan shells. *J. Geol.* 101:729–747.
- Green, M. A. & R. C. Aller. 1998. Seasonal patterns of carbonate diagenesis in nearshore terrigenous muds: relation to spring phytoplankton bloom and temperature. *J. Mar. Res.* 56:1097–1123.
- Green, M. A. & R. C. Aller. 2001. Early diagenesis of calcium carbonate in Long Island Sound sediments: benthic fluxes of Ca<sup>2+</sup> and minor elements during seasonal periods of net dissolution. *J. Mar. Res.* 59:769–794.
- Green, M. A., G. G. Waldbusser, L. Hubazc, E. Cathcart & J. Hall. Carbonate mineral saturation state as the recruitment cue for settling bivalves in marine muds. *Estuaries Coasts.*
- Green, M. A., G. G. Waldbusser, S. L. Reilly, K. Emerson & S. O'Donnell. 2009. Death by dissolution: sediment saturation state as a mortality factor for juvenile bivalves. *Limnol. Oceanogr.* 54:1037–1047.
- Gutierrez, J. L., C. G. Jones, D. L. Strayer & O. O. Iribarne. 2003. Mollusks as ecosystem engineers: the role of shell production in aquatic habitats. *Oikos* 101:79–90.
- Gypens, N., A. V. Borges & C. Lancelot. 2009. Effect of eutrophication on air–sea CO<sub>2</sub> fluxes in the coastal southern North Sea: a model study of the past 50 years. *Glob. Change Biol.* 15:1040–1056.
- Hales, B. & S. Emerson. 1997. Evidence in support of first-order dissolution kinetics of calcite in seawater. *Earth Planet. Sci. Lett.* 148:317–327.
- Harding, J. M., R. Mann, M. J. Southworth & J. A. Wesson. 2010. Management of the Piankatank River, Virginia, in support of oyster (*Crassostrea virginica*, Gmelin 1791) fishery repletion. *J. Shellfish Res.* 29:867–888.
- Hargis, W. J. & D. S. Haven. 1999. Chesapeake oyster reefs: Their importance, destruction, and guidelines for restoring them. In: M. W. Luckenbach, R. Mann & J. A. Wesson, eds. Oyster reef habitat restoration: A synopsis and synthesis of approaches. Gloucester, VA: Virginia Institute of Marine Science Press. 372 pp.
- Hautmann, M. 2006. Shell mineralogical trends in epifaunal Mesozoic bivalves and their relationship to seawater chemistry and atmospheric carbon dioxide concentration. *Facies* 52:417–433.
- Hecht, F. 1933. Der Verbleib der organische Substanz der Tiere bei meerischer Einbettung. *Senckenb. Biol.* 15:165–219.
- Honjo, S. & J. Erez. 1978. Dissolution rates of calcium carbonate in deep ocean: *in situ* experiment in North Atlantic Ocean. *Earth Planet. Sci. Lett.* 40:287–300.
- Hopkins, S. H. 1962. Distribution of species *Cliona* (boring sponge) on the eastern shore of Virginia in relation to salinity. *Chesap. Sci.* 2:121–124.
- Hu, X., W. J. Cai, Y. Wang, X. Guo & S. Luo. 2011. Geochemical environments of continental shelf: upper slope sediments in the northern Gulf of Mexico. *Palaeogeogr. Palaeoclimatol. Palaeoecol.*
- Kelly, R. P., M. M. Foley, W. S. Fisher, R. A. Feely, B. S. Halpern, G. G. Waldbusser & M. R. Caldwell. 2011. Mitigating local causes of ocean acidification with existing laws. *Science* 332:1036–1037.
- Kidwell, S. M. 2005. Shell composition has no net impact on large-scale evolutionary patterns in mollusks. *Science* 307:914–917.
- Kidwell, S. M. & D. Jablonski. 1983. Taphonomic feedback: ecological consequences of shell accumulation. In: M. J. S. Tevesz & P. L. McCall, editors. Biotic interactions in recent and fossil benthic communities. New York: Plenum Press. pp. 195–248.
- Kimmel, D. G. & R. I. E. Newell. 2007. The influence of climate variation on Eastern oyster (*Crassostrea virginica*) juvenile abundance in Chesapeake Bay. *Limnol. Oceanogr.* 52:959–965.

- Kobluk, D. R. & M. J. Risk. 1977. Calcification of exposed filaments of endolithic algae, micrite envelope formation and sediment production. *J. Sediment. Petrol.* 47:517–528.
- Lebrato, M., D. Iglesias-Rodriguez, R. A. Feely, D. Greeley, D. O. B. Jones, N. Suarez-Bosche, R. S. Lampitt, J. E. Cartes, D. R. H. Green & B. Alker. 2010. Global contribution of echinoderms to the marine carbon cycle: CaCO<sub>3</sub> budget and benthic compartments. *Ecol. Monogr.* 80:441–467.
- Longman, M. W. 1980. Carbonate diagenetic textures from near-surface diagenetic environments. *AAPG Bull. Am. Assoc. Petrol. Geologists* 64:461–487.
- Mann, R. & E. N. Powell. 2007. Why oyster restoration goals in the Chesapeake Bay are not and probably cannot be achieved. *J. Shellfish Res.* 26:905–917.
- Mannino, A. & H. R. Harvey. 1999. Lipid composition in particulate and dissolved organic matter in the Delaware Estuary: sources and diagenetic patterns. *Geochim. Cosmochim. Acta* 63:2219–2235.
- Miller, A. W., A. C. Reynolds, C. Sorbino & G. F. Riedel. 2009. Shellfish face uncertain future in high CO<sub>2</sub> world: influence of acidification on oyster larvae calcification and growth in estuaries. *PLoS Biol.* 4:e5661.
- Millero, F. J., T. B. Graham, F. Huang, H. Bustos-Serrano & D. Pierrot. 2006. Dissociation constants of carbonic acid in seawater as a function of salinity and temperature. *Mar. Chem.* 100:80–94.
- Morse, J. W. 2005. Formation and diagenesis of carbonate sediments. In: F. T. Mackenzie, editor. *Sediments, diagenesis, and sedimentary rocks*. Oxford: Elsevier-Pergamon. pp. 67–86.
- Morse, J. W. & R. S. Arvidson. 2002. The dissolution kinetics of major sedimentary carbonate minerals. *Earth Sci. Rev.* 58:51–84.
- Morse, J. W., R. S. Arvidson & A. Lutge. 2007. Calcium carbonate formation and dissolution. *Chem. Rev.* 107:342–381.
- Morse, J. W. & W. H. Casey. 1988. Ostwald processes and mineral paragenesis in sediments. *Am. J. Sci.* 288:537–560.
- Najjar, R. G., C. R. Pyke, M. B. Adams, D. Breitburg, C. Hershner, M. Kemp, R. Howarth, M. R. Mulholland, M. Paolisso, D. Secor, K. Sellner, D. Wardrop & R. Wood. 2010. Potential climate-change impacts on the Chesapeake Bay. *Estuar. Coast. Shelf Sci.* 86:1–20.
- Palma, R. M., G. S. Bressan & D. A. Kietzmann. 2008. Diagenesis of a bioclastic oyster deposit from the Lower Cretaceous (Chachao Formation), Neuquen Basin, Mendoza Province, Argentina. *Carbonates Evaporites* 23:39–49.
- Pomponi, S. A. & D. W. Meritt. 1990. Distribution and life history of the boring sponge *Cliona truttii* in the upper Chesapeake Bay. In: K. Rutzler, editor. *New perspectives in sponge biology*. Washington, DC: Smithsonian Institution Press. pp. 384–390.
- Pouchou, J. L. & F. Pichoir. 1984. A new model for quantitative X-ray microanalysis. 1. Application to the analysis of homogeneous samples. *Recherche Aerospatiale* 3:167–192.
- Powell, E. N., C. E. Brett, K. M. Parsons-Hubbard, W. R. Callender, G. M. Staff, S. E. Walker, A. Raymond & K. A. Ashton-Alcox. 2011a. The relationship of bionts and taphonomic processes in molluscan taphofacies formation on the continental shelf and slope: eight-year trends: Gulf of Mexico and Bahamas. *Facies* 57:15–37.
- Powell, E. N., J. N. Kraeuter & K. A. Ashton-Alcox. 2006. How long does oyster shell last on an oyster reef? *Estuar. Coast. Shelf Sci.* 69:531–542.
- Powell, E. N. & J. M. Klinck. 2007. Is oyster shell a sustainable estuarine resource? *J. Shellfish Res.* 26:181–194.
- Powell, E. N., G. M. Staff, W. R. Callender, K. A. Ashton-Alcox, C. E. Brett, K. M. Parsons-Hubbard, S. E. Walker & A. Raymond. 2011b. Taphonomic degradation of molluscan remains during thirteen years on the continental shelf and slope of the northwestern Gulf of Mexico. *Palaeogeogr. Palaeoclimatol. Palaeoecol.* [in press].
- Rosell, D., M. J. Uriz & D. Martin. 1999. Infestation by excavating sponges on the oyster (*Ostrea edulis*) populations of the Blanes littoral zone (north-western Mediterranean Sea). *J. Mar. Biol. Assoc. UK* 79:409–413.
- Rude, P. D. & R. C. Aller. 1991. Fluorine mobility during early diagenesis of carbonate sediments: an indicator of mineral transformations. *Geochim. Cosmochim. Acta* 55:2491–2509.
- Salisbury, J., M. A. Green, C. Hunt & J. Campbell. 2008. Coastal acidification by rivers: a threat to shellfish? *Eos Trans. AGU* 89:513–514.
- Schulte, D. M., R. P. Burke & R. N. Lipcius. 2009. Unprecedented restoration of a native oyster metapopulation. *Science* 325:1124–1128.
- Southworth, M., J. M. Harding, J. A. Wesson & R. Mann. 2010. Oyster (*Crassostrea virginica*, Gmelin 1791) population dynamics on public reefs in the Great Wicomico River, Virginia, USA. *J. Shellfish Res.* 29:271–290.
- van Heuven, S., D. Pierrot, J. W. B. Rae, E. Lewis & D. W. R. Wallace. 2011. MATLAB Program Developed for CO<sub>2</sub> System Calculations. ORNL/CDIAC-105b. Carbon Dioxide Information Analysis Center, Oak Ridge National Laboratory, U.S. Department of Energy, Oak Ridge, Tennessee. DOI: 10.3334/CDIAC/otg.CO2SYS\_MATLAB\_v1.1.
- Waldbusser, G. G., H. Bergschneider & M. A. Green. 2010. Size-dependent pH effect on calcification in post-larval hard clam *Mercenaria* spp. *Mar. Ecol. Prog. Ser.* 417:171–182.
- Waldbusser, G. G., E. P. Voigt, H. Bergschneider, M. A. Green & R. I. E. Newell. 2011. Biocalcification in the Eastern oyster (*Crassostrea virginica*) in relation to long-term trends in Chesapeake Bay pH. *Estuaries Coasts* 34:221–231.
- Walter, L. M. & J. W. Morse. 1984. Reactive surface-area of skeletal carbonates during dissolution: effect of grain-size. *J. Sediment. Petrol.* 54:1081–1090.
- Zondervan, I., R. E. Zeebe, B. Rost & U. Riebesell. 2001. Decreasing marine biogenic calcification: a negative feedback on rising atmospheric pCO<sub>2</sub>. *Global Biogeochem. Cycles* 15:507–516.
- Zuschin, M., M. Stachowitsch & R. J. Stanton. 2003. Patterns and processes of shell fragmentation in modern and ancient marine environments. *Earth Sci. Rev.* 63:33–82.